

Damage detection of reinforced concrete columns retrofitted with FRP jackets by using PZT sensors

Efi A. Tzoura^{*1}, Thanasis C. Triantafyllou^{1a}, Costas Providakis^{2b},
Aristomenis Tsantilis^{1c}, Corina G. Papanicolaou^{1d} and Dimitris L. Karabalis^{1e}

¹Department of Civil Engineering, University of Patras, GR-26500 Patras, Greece

²Department of Architectural Engineering, Technical University of Crete, GR-73100 Chania, Greece

(Received August 29, 2014, Revised May 15, 2015, Accepted May 20, 2015)

Abstract. In this paper lead zirconate titanate transducers (PZT) are employed for damage detection of four reinforced concrete (RC) column specimens retrofitted with carbon fiber reinforced polymer (CFRP) jackets. A major disadvantage of FRP jacketing in RC members is the inability to inspect visually if the concrete substrate is damaged and in such case to estimate the extent of damage. The parameter measured during uniaxial compression tests at random times for known strain values is the real part of the complex number of the Electromechanical Admittance (Conductance) of the sensors, obtained by a PXI platform. The transducers are placed in specific positions along the height of the columns for detecting the damage in different positions and carrying out conclusions for the variation of the Conductance in relation to the position the failure occurred. The quantification of the damage at the concrete substrate is achieved with the use of the root-mean-square-deviation (RMSD) index, which is evaluated for the corresponding strain values. The experimental results provide evidence that PZT transducers are sensitive to damage detection from an early stage of the experiment and that the use of PZT sensors for monitoring and detecting the damage of FRP-retrofitted reinforced concrete members, by using the Electromechanical Admittance (EMA) approach, can be a highly promising method.

Keywords: damage detection; electromechanical admittance; FRP jackets; PZT transducers; reinforced concrete

1. Introduction

For over a century reinforced concrete (RC) is the most prevalent composite material used in structures. Although RC has been proved to be a durable material through time, in recent years several structures need to be rehabilitated. Deterioration of old structures due to aging and/or the need to upgrade existing structures, e.g., as a means of seismic retrofitting, leads nowadays to the

*Corresponding author, Ph.D. Student, E-mail: eficivil@yahoo.gr

^a Professor, E-mail: ttriant@upatras.gr

^b Professor, E-mail: cprov@mred.tuc.gr

^c Ph.D. Student, E-mail: tsantilis.info@gmail.com

^d Assistant Professor, E-mail: kpapanic@upatras.gr

^e Professor, E-mail: karabali@upatras.gr

solution of retrofitting with various methods.

During the last decades the revolutionary method of fiber reinforced polymer (FRP) jacketing has been proposed for flexural strengthening, shear strengthening and confinement of RC (e.g., Triantafillou 2001). Due to the high strength-to-weight ratio and the ease of their application, FRP jackets have become quite popular and have been used in several structures; the FRP jacketing technique has proved to be quite efficient.

Although utilization of FRP as a strengthening technique is widespread with a great amount of research being carried out in this field, a particular drawback of this method is its inability to allow detection of possible damage on the reinforced concrete substrate over time, compared to other strengthening techniques, e.g. reinforced concrete (RC) jackets or textile reinforced mortar (TRM) jackets.

In past studies, methods of Structural Health Monitoring (SHM) have been proposed, which mainly concern damage detection techniques (e.g., Davor and Richard 1998, Giurgiutiu *et al.* 2003, Akuthota *et al.* 2004, Kim *et al.* 2007), aiming to reduce the inspection cost of structures. Nevertheless, each of these traditional damage detection techniques has their positive and negative virtues. Furthermore, many traditional techniques require out of service periods or can be applied only a certain time intervals. Another drawback of these traditional techniques is the need to know in advance the area where the damage will occur and that the specific area can be easily accessible. Among them, the acoustic emission technique is suitable for long-term and in-service monitoring but needs to filter out the noise from the emission signals (Peairs *et al.* 2003).

The existing SHM methods applied on FRP jackets concern the detection of the debonding of FRP sheets or laminates from concrete members either experimentally or analytically (Saafi and Sayyah 2000, Oehlers 2004). To the best of our knowledge none of them concerns damage detection of the concrete substrate, when failure occurs due to (brittle) FRP rupture. Before rupture occurs the possible cracks at the concrete substrate cannot be inspected visually. None of the contemporary non-destructive damage detection methods has proved to be appropriate for reliable conclusions in such cases. Furthermore, the continuous monitoring of structures with the usual methods has the significant disadvantages mentioned above.

Nowadays Lead Zirconate Titanate (PZT) transducers are widely used for damage detection in steel and reinforced concrete structures (Bhalla and Soh 2003, 2004). The advantage of the PZT transducers over the two other methods (strain tracking and acoustic emission) is due to the low cost of the equipment, the simplicity in applying them and the low storage space required. PZT transducers use the piezoelectric effect to measure changes in strain by converting them to an electrical charge and conversely when applying an electric field to measure the mechanical strain. Consequently a PZT transducer can be used both as an actuator and as a sensor.

Damage detection on the basis of measuring the electromechanical admittance (EMA) of PZT transducers was proposed by Liang *et al.* (1994). Techniques concerning the EMA measurements have also been proposed by Park *et al.* (2006a, 2006b, 2009) and Overly *et al.* (2009). The main advantages of this technique are the ability to detect damage in small and large scale, the potential for continuous on-line monitoring, the low cost and the ease of practical application. The electromechanical admittance of the transducers is directly related to the electromechanical admittance of the structure. When cracks propagate in a reinforced concrete member, the electromechanical admittance undergoes changes. These changes are the main indicator for damage detection. So far only a few number of studies utilized the EMA approach for structural health monitoring of structures retrofitted with FRP (Kim *et al.* 2008, Park *et al.* 2011, Providakis *et al.* 2013).

The Root-Mean-Square-Deviation (RMSD) function has been proposed for quantifying the damage of the concrete substrate with respect to the changes of the admittance; this function is regarded as a reliable damage index (Tseng and Naidu 2001, Yang *et al.* 2008).

In the present study PZT transducers are used for damage detection of reinforced concrete columns strengthened with FRP jackets, in order to detect damage of the concrete substrate. The PZT transducers are externally placed on the FRP jacket and the electromechanical admittance is measured during the experiment as the damage propagates. The variation of the real part of the admittance (conductance) is used for quantifying the damage in combination with the statistical root-mean-square-deviation index.

2. Electromechanical admittance (EMA) approach

The measure of the electromechanical admittance of the specimens was based on a I-V method developed on a PCI eXtensions for Instrumentation (PXI) platform setup to generate, acquire and elaborate a sine wave in the range of predefined frequencies $f(=\omega/2\pi)$ between 100 and 250 kHz. In the I-V method, an unknown admittance Y over the PZT surfaces can be calculated from the measured voltage V and current I by taking into account the ratio $I(\omega)/V(\omega)$. Current is calculated using the voltage measurements across an accurately known low value resistor R_c . The I-V circuit which is utilized in this work is similar to a voltage divider and schematically is presented in diagram of Fig. 1 A function generator (F.G.) outputs a sinusoidal excitation $V_{in}=V_o.\sin(\omega t)$ within the predefined frequency range. The sinusoidal excitation is normally limited to a small level so that the current response $I=I_o.\sin(\omega t+\phi)$ across the PZT surfaces and the resistor R_c will be a sinusoid at the same frequency $\omega(=2\pi f)$ but shifted in phase ϕ with I_o being the amplitude of the current response. The DAQ card of PXI platform setup records simultaneously the voltage V_{in} at the output of the function generator and the voltage drop V_R on the calibrated resistor. Hence, since the PZT admittance Y is given by $Y=I/(V_{in}-V_R)=V_R/(V_{in}-V_R)*R_c$, the unknowns are the complex voltages V_R and $(V_{in}-V_R)$.

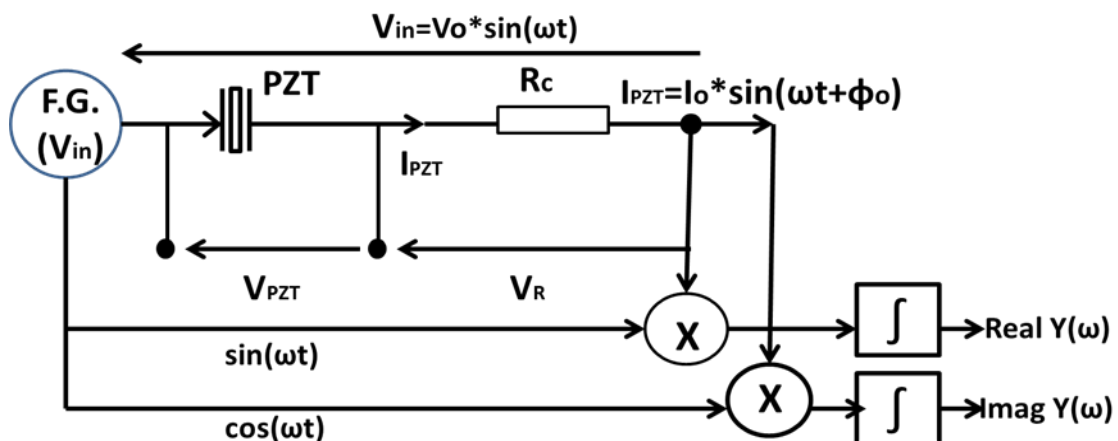


Fig. 1 Functional diagram for the admittance measuring system setup

Several possible methods exist for computing the unknown complex voltages after the voltage-current signals have been obtained. In this work one of the most widely used techniques, the integration or sine correlation method, is utilized which is also depicted as a complementary part of the diagram in Fig. 1. In sine correlation method, the measured current I is multiplied by the in-phase (sine) and in-quadrature (cosine) signals at the same frequency ω and then is integrated during one ($cyc=1$) or more ($cyc>1$) complete wave periods $T=1/f=2\pi/\omega$ of the sinusoidal wave signal. Finally, the real (conductance) and imaginary (susceptance) parts of admittance Y in the range of the predefined frequency band are calculated (with respect to frequency ω) according to the following integrals (Giurgiutiu and Xu 2004)

$$\text{Real part of admittance } G: \frac{2}{cyc * T} \int_0^{cyc * T} I_0 * \sin(\omega \cdot t + \varphi) * \sin(\omega \cdot t) dt \quad (1)$$

$$\text{Imaginary part of admittance } B: \frac{2}{cyc * T} \int_0^{cyc * T} I_0 * \sin(\omega \cdot t + \varphi) * \cos(\omega \cdot t) dt \quad (2)$$

Hence the electromechanical admittance is given by the following equation

$$\bar{Y} = G + Bj \quad (3)$$

Assuming that the mechanical property of PZT transducers does not vary over the monitoring period T it has been proved (Giurgiutiu and Xu 2004) that the PZT electrical impedance (or admittance) is directly related to the mechanical impedance of the investigated host structure and thus any variations in the electrical impedance (admittance) can be considered as an indication of changes in structural integrity. Since the electrical admittance is primarily capacitive, the real part G plays a dominant role to the final value of admittance as computed from Eq. (1). Taking also into account that the imaginary part B is more sensitive to the temperature variations, we easily reach to the conclusion that damage mainly affects the real part G of PZT electrical admittance. Therefore, the conductance (G) is the determinant quantity in the current study in order to compare its measure at healthy and damaged state for quantifying the damage, as mentioned above.

3. Experimental program

A total of four reinforced concrete column specimens were tested in axial loading with three PZT transducers placed along the height of each column. A description of the specimens follows next, supported by Fig. 2:

- Specimen II3C was retrofitted with two layers of carbon fiber reinforced polymer (CFRP) jacket without anchors, having a rectangular cross-section of 450x150 mm.
- Specimen II4C was retrofitted with two layers of CFRP jacket without anchors, having a rectangular cross-section of 600x150 mm.
- Specimen IIIA3C was retrofitted with three layers of CFRP jacket with anchors, having a rectangular cross-section of 450x150 mm.
- Specimen IIIA4C was retrofitted with three layers of CFRP jacket with anchors, having a rectangular cross-section of 600x150 mm.

Note that these specimens form a sub-group of large group of specimens tested to investigate the effectiveness of different CFRP confining schemes on columns with large cross sectional aspect ratios (3:1 and 4:1).

Casting of the specimens was made with the same batch of ready-mix concrete in stiff moulds.

The average compressive strength at the time of testing of the columns (10 months after casting), measured on 150x150 mm cubes was 21 MPa. Strength properties (average values from three specimens) for the steel used for longitudinal and transverse reinforcement were as follows: yield stress 570 MPa, tensile strength 680 MPa. A few days (two to four) before testing, all specimens were capped with a special self-leveling high-strength mortar. Capping is necessary for all specimens subjected to compression (axial load) in order to achieve a uniform and flat surface for the load to be applied.

The carbon fiber sheet used for confinement was a commercial unidirectional fiber product with a weight of 644 g/m². The carbon fiber sheet was impregnated with a commercial low viscosity structural adhesive (two-part epoxy resin with a mixing ratio 3:1 by weight) with tensile strength of 72.4 MPa and an elastic modulus of 3.2 GPa (cured three days at 60°C). Values of tensile strength and elastic modulus for one layer of the epoxy-impregnated carbon sheet from manufacturer data sheets were equal to 986 MPa and 95.8 GPa, respectively, corresponding to a nominal thickness equal to 1 mm. These values were confirmed by testing five coupons in uniaxial tension according to EN 2561 (1995). The test results gave an average tensile strength equal to 1046 MPa and an elastic modulus equal to 93.7 GPa.

Each anchor comprised a tow of fibers of the same type used in the unidirectional sheets. The length of anchors was 350 mm and their weight was 30 g/m. Impregnation and bonding of fiber anchors was done using the same epoxy adhesive used for the impregnation of the carbon sheets.

The anchors were inserted into holes through the thickness of each specimen along the height, following the application of the FRP jacket. They were spread on both sides in a fan shape and in the end they were covered with an additional strip of fabric. The configuration of the anchors is shown in Figs. 2(a) and 1(b) for specimens IIIA3C and IIIA4C.

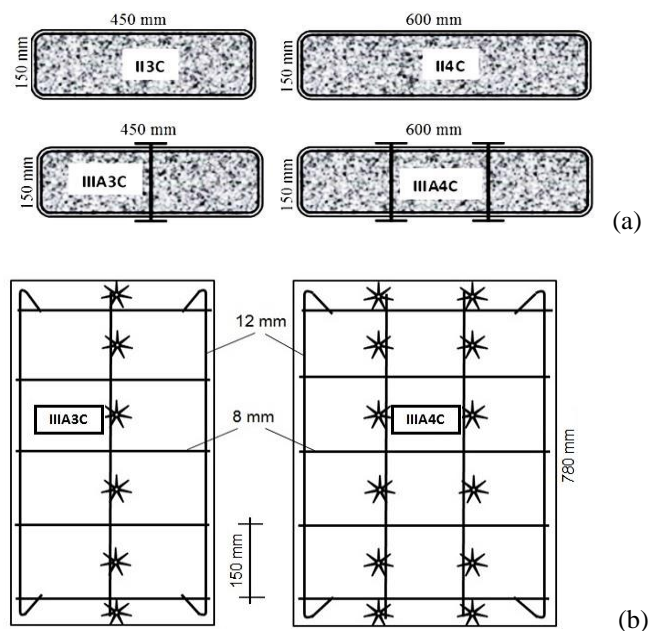


Fig. 2 Geometry of specimens: (a) Cross section, (b) elevation

All specimens were subjected to uniaxial compression and failed due to CFRP rupture either at the top or at the bottom of the specimen, near the corners, due to stress concentrations in the jacket. For specimens II3C and IIIA3C the jacket failed at the top and for specimens II4C and IIIA4C the CFRP jacket failed at the bottom (Fig. 3).

The PZT transducers had a thickness of 2 mm and a width, equal to the height, of 10 mm. The arrangement of the transducers along the height of the specimens is shown in Fig. 4 (dimensions in mm). The notation of the transducers is PZT_u for the transducer placed at the upper part of the specimen, PZT_l for the one placed at the lower part of the specimen and PZT_b for the one placed in between. The free PZT surfaces were sealed by using a Dow Corning RTV 3140 (Dow Corning) coating silicon elastomer film appropriate to protect from PZT corrosion and ageing effect.

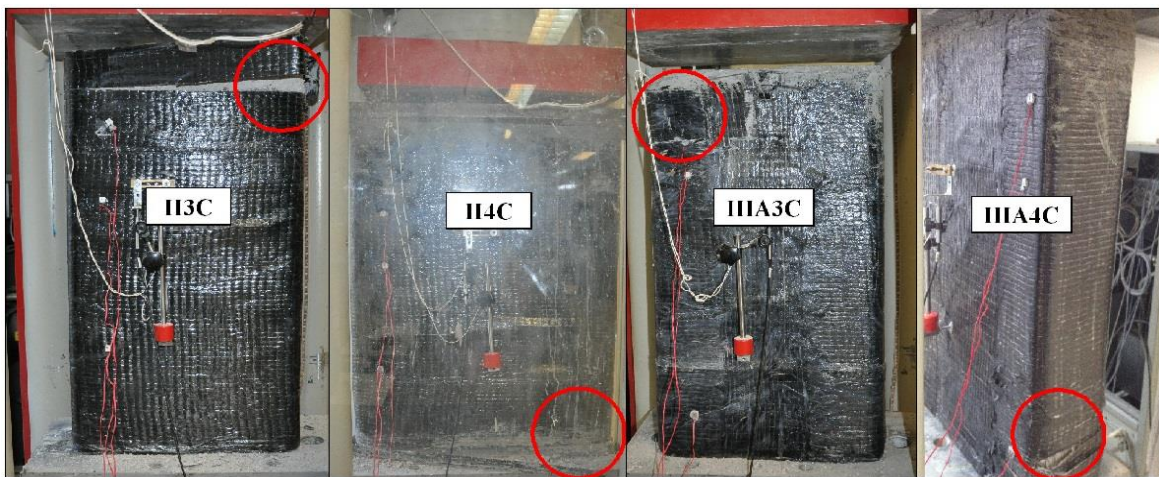


Fig. 3 FRPrupture

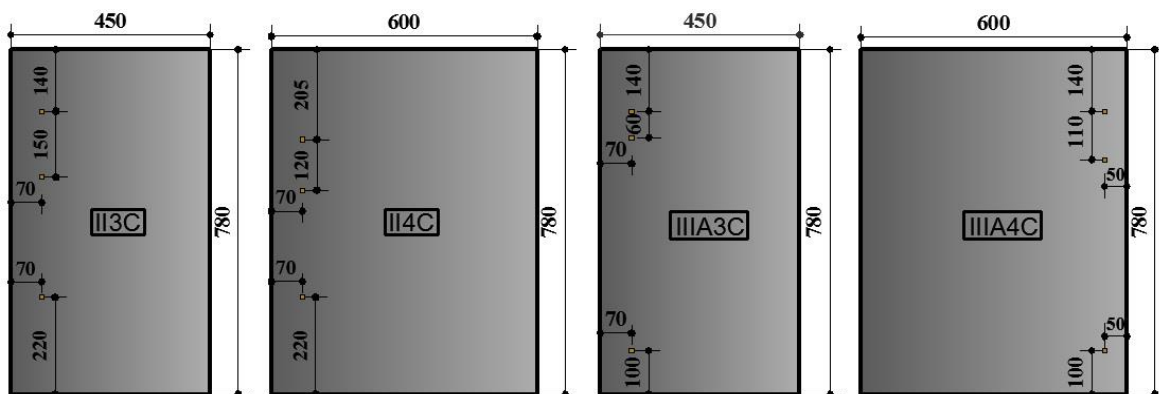


Fig. 4 Arrangement of PZT transducers (dimensions in mm)

Table 1 Properties of PZT transducers

Property	Remarks
Density	7.80 (g/cm ³)
Electric Permittivity $\epsilon_{33}^T/\epsilon_0$	1750
Piezoelectric Strain Coefficient d_{31}	-180 (10 ⁻¹² C/N)
Elastic Compliance Coefficients S_{11}^E	16.1 (10 ⁻¹² m ² /N)
S_{33}^E	20.7 (10 ⁻¹² m ² /N)
Dielectric loss factor $\tan\delta(10^{-3})$	20

As shown in Fig. 4, for specimens IIIA3C and IIIA4C transducers were placed in the area where FRP rupture occurred. For specimens II3C and II4C the nearest PZT transducer in the area where FRP rupture occurred was placed in a distance of 70 mm and 170 mm, respectively.

The main properties of the PZT transducers are presented in Table 1, as provided by data sheets of the manufacturer. The PZT transducers were used autonomously as wave transmitters and receivers at the same time.

4. Experimental results and discussion

As mentioned above the electromechanical admittance of the PZT sensors was obtained during the experimental procedure for various strain values. The measure used for damage detection is the real part of the complex number of the electromechanical admittance (Conductance). From the stress-strain curves given in Fig. 5 it can be seen that for the specimens with the three layers of CFRP jacket the peak load is reached for higher values of strain than for the specimens with two layers. Hence the damage for specimens II3C and II4C must had started at an earlier stage (for lower values of strain) than for the other two specimens.

Figs. 6-17 illustrate subplots of the Conductance measures with respect to Frequency for specific values of strain. Instead of illustrating the graphs for all frequency values and the corresponding Conductance values, subplots are presented for a subspace of frequency values near the first resonant frequency, where the most significant variations of the Conductance were recorded.

At the beginning of the experiment (healthy state) the strain is equal to zero. As the axial load increases, cracks are created at the concrete substrate. Consequently the admittance of the concrete member changes as the cracks propagate. In the graphs of Conductance-Frequency at the resonant frequencies (about 160-165 kHz) where conductance reaches its maximum values (peaks), the variation of its value for various values of strain, is notably visible. This variation is associated with the damage of the specimens.

The damage detection is quantified by calculating the normalized root-mean-square-deviation (RMSD) and can be used as a damage index. The RMSD value of the i^{th} measurement G_i with respect to the initial measurement G_0 of the conductance is defined as

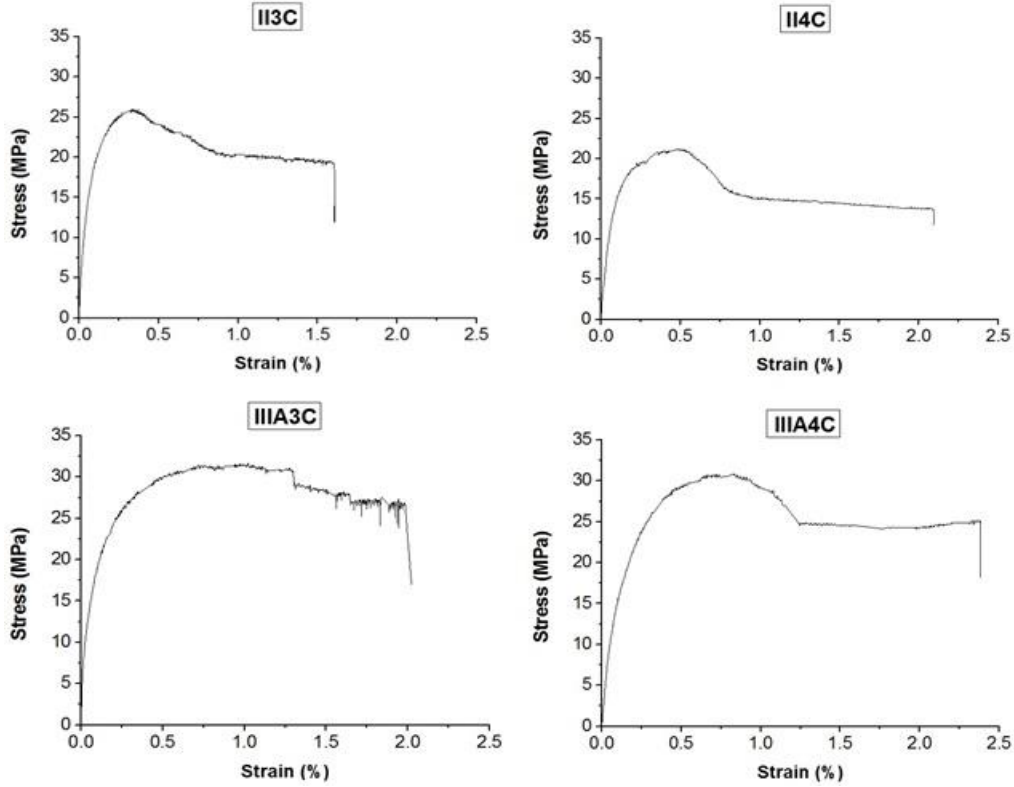


Fig. 5 Stress-strain curves

$$RMSD = \sqrt{\frac{\sum_{i=0}^n (G_0 - G_i)^2}{\Sigma(G_0)^2}} \quad (4)$$

Fig. 18 illustrates the RMSD value as defined in the previous equation for each measurement during the experiment and for each PZT transducer.

The admittance can be either increasing or decreasing. The peaks of the admittance at the resonant frequencies just indicate the dynamic behavior of the system PZT-structure. The measurements of the current flow depend on the strain developed on the PZT. When damage occurs, the dynamic behavior of the system PZT – structure, changes. After cracks are formed, at the beginning of the experiment, it is likely to observe decrease of the admittance, for example because of compression of the two sides of the crack, but as the cracks propagate and their width increases, the admittance will be increasing. Furthermore when a structure is strengthened with FRP jacket, as the strain increases, the behavior of the current flow will be different after the debonding of the FRP jacket. In Fig. 6 relating to PZT_u for Specimen II3C, the peak value of the real part of the admittance (Conductance) gradually decreases for strain values up to 0.14%. In Figs. 7 and 8 counterpart graphs are given for PZT_b and PZT_1. The curves of Conductance-Frequency for PZT_b and PZT_u indicate small variations proving that the

transducer located at least 150 mm far from PZT_u exhibits different behavior with transducer PZT_u. Thus, the signature of the admittance of PZT_u located in the vicinity of the FRP rupture was found to have undergone drastic changes while the second and the third PZT placed in between (PZT_b) and at the lower part of the specimen (PZT_l), respectively, fail to detect damage, as they are located far from the area where the FRP rupture occurred. In Figs. 9-17 the Conductance-Frequency graphs are presented for the other three specimens.

The graphs regarding Specimen II4C confirm the behavior of the PZT transducers observed for Specimen II3C. As mentioned above, the FRP jacket rupture for Specimen II4C occurred at the lower part of it. The nearest transducer PZT_1 was located 170 mm far from the area of the FRP rupture (220 mm far from the bottom of the specimen).

For the specimens strengthened with three layers of FRP, the transducers placed near the area where the FRP rupture occurred (PZT_u for Specimen IIIA3C and PZT_1 for Specimen IIIA4C), gave similar recordings. The Conductance increases at the beginning and starts to decrease for strain values corresponding to load values close to the peak load.

It is clear that for the specimens strengthened with two layers of FRP jacket, when a PZT transducer is placed to a close distance (maximum 170 mm in this study), it can detect the damage of the concrete substrate at an early stage. For the specimens strengthened with three layers of FRP jacket, the PZT transducers used fail to detect the damage of the concrete substrate.

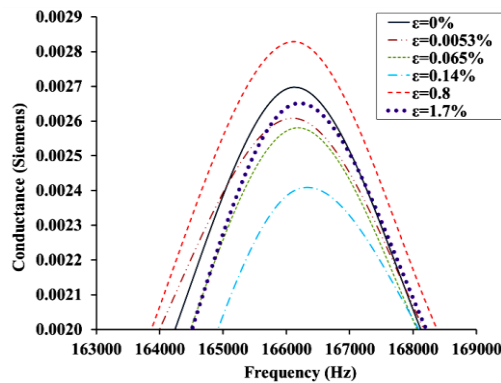


Fig. 6 Conductance versus frequency, Specimen II3C-PZT_u

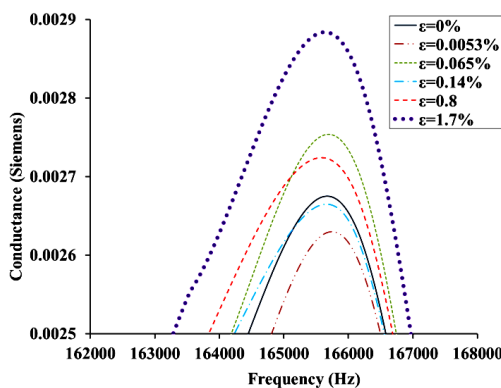


Fig. 7 Conductance versus frequency, Specimen II3C-PZT_b

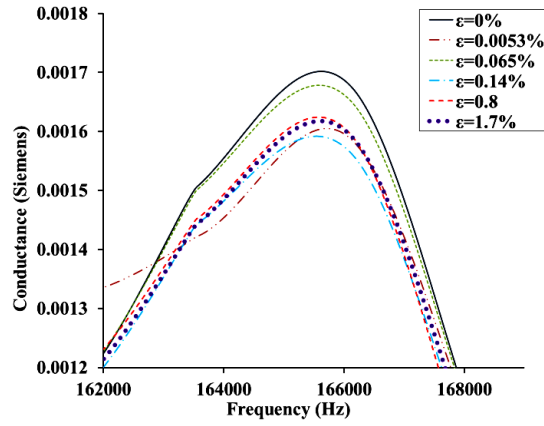


Fig. 8 Conductance versus frequency, Specimen II3C-PZT_1

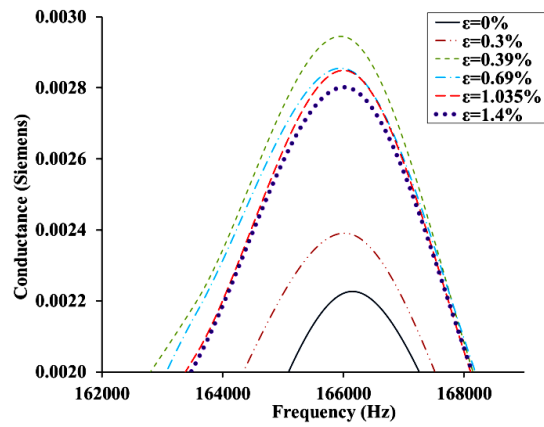


Fig. 9 Conductance versus frequency, Specimen II4C-PZT_u

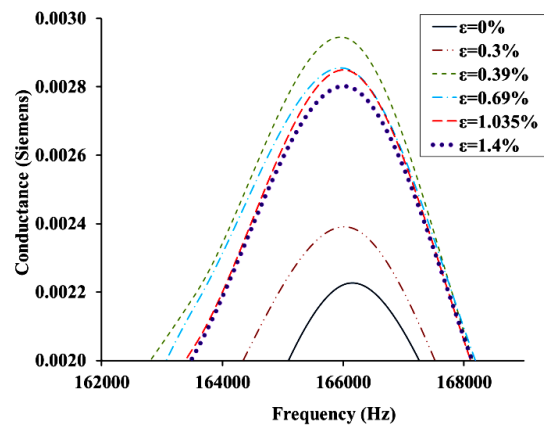


Fig. 10 Conductance versus frequency, Specimen II4C-PZT_b

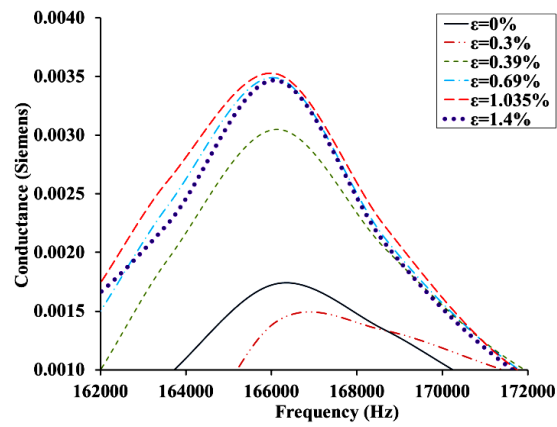


Fig. 11 Conductance versus frequency, Specimen II4C-PZT_1

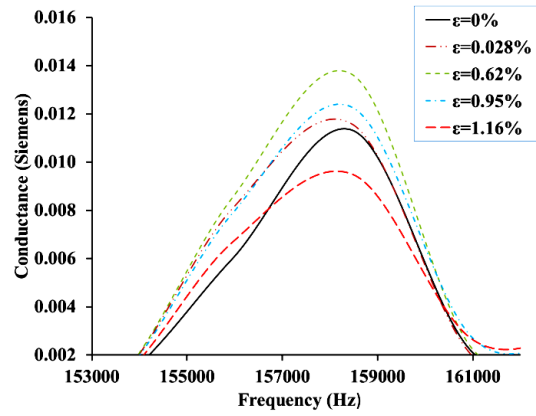


Fig. 12 Conductance versus frequency, Specimen IIIA3C-PZT_u

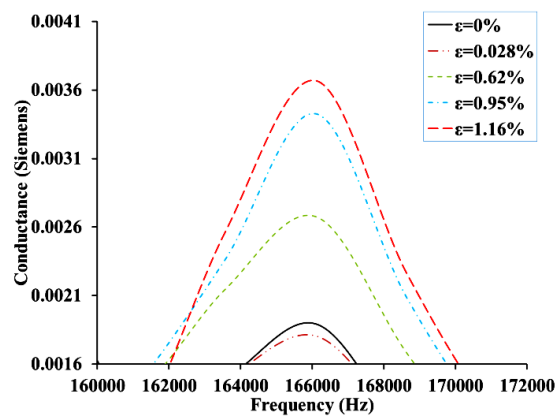


Fig. 13 Conductance versus frequency, Specimen IIIA3C-PZT_b

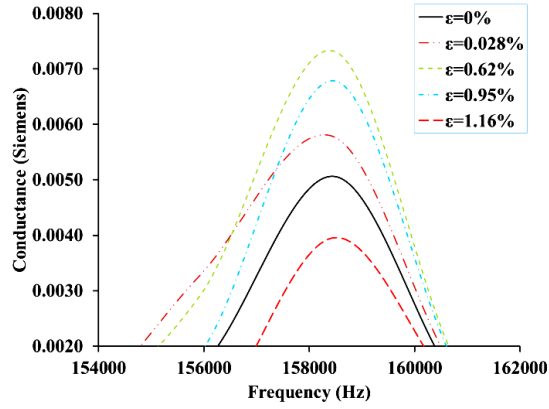


Fig. 14 Conductance versus frequency, Specimen IIIA3C-PZT_1

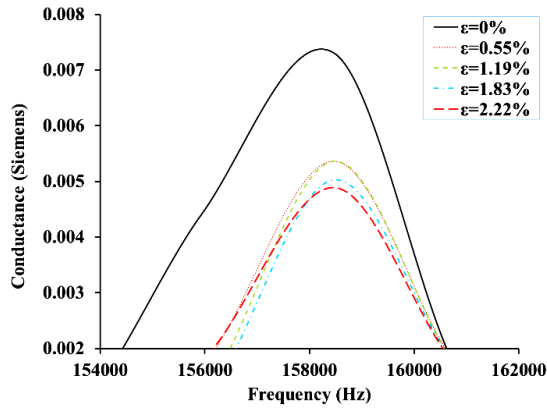


Fig. 15 Conductance versus frequency, Specimen IIIA4C-PZT_u

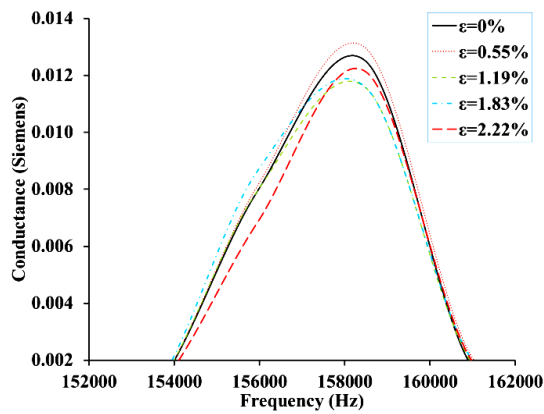


Fig. 16 Conductance versus frequency, Specimen IIIA4C-PZT_b

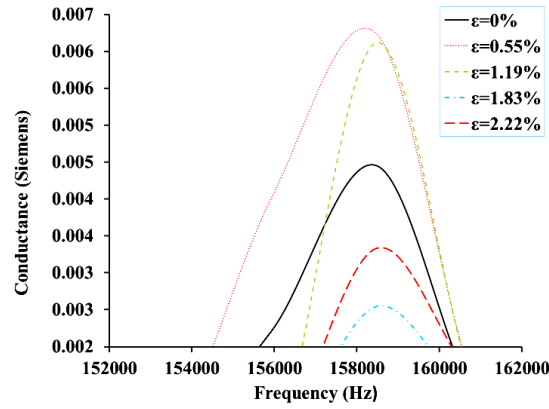


Fig. 17 Conductance versus frequency, Specimen IIIA4C-PZT_1

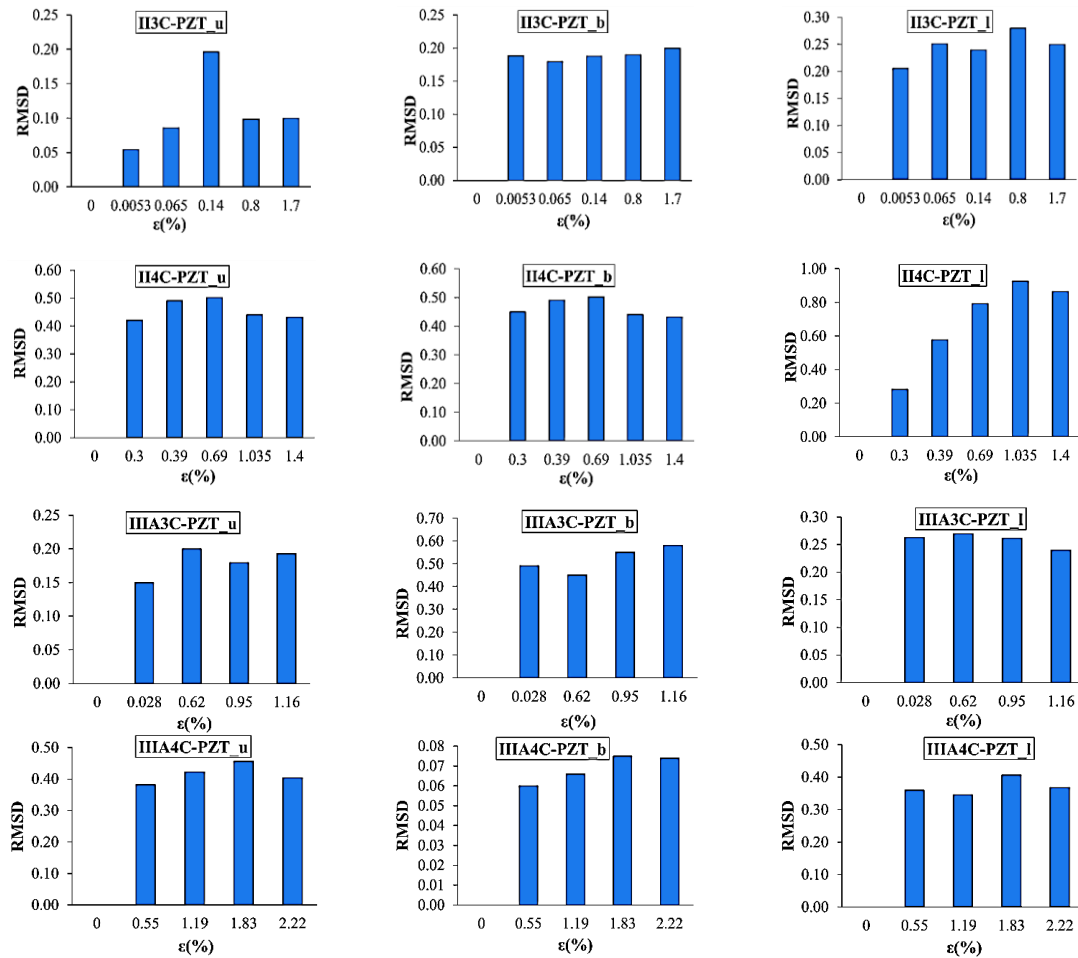


Fig. 18 RMSD versus strain

Table 2 Maximum stress and corresponding strain value

Specimen	Maximum stress(MPa)	Strain (%)
II3C	25.99	0.375
II4C	21.24	0.49
IIIA3C	31.68	1.02
IIIA4C	30.87	0.83

The strain values for which the Conductance is illustrated in Figs. 6-17 represent a significant proportion of the strain value that corresponds to the peak load and consequently to the maximum stress. The maximum stress value for each specimen is presented in Table 2.

As already mentioned above, the quantification of the damage is achieved by using the root-mean-square-deviation (RMSD) index. In Fig. 18 the RMSD index is calculated for the same strain values as the Conductance. The variations of the RMSD index is wider for the transducers placed near the damage area as expected for the specimens strengthened with two layers of FRP jackets. For the specimens strengthened with three layers of FRP jacket there is no consistent behavior though. The most significant variations of the RMSD index value are observed for the transducers placed between the upper and lower transducers. In the middle area of the height of the specimens the dilation behavior of the FRP jacket is observed for column specimens subjected to compressive axial load. Hence the deformation of the FRP jackets is visible and obtains high values.

Because the area where the FRP fracture would occur was not known in advance, the transducers were placed in various positions. The distance between the transducers PZT_u and PZT_b is smaller than the distance the transducers PZT_l were placed from PZT_u and PZT_b. Therefore a comparison would be meaningful only for the transducers PZT_u and PZT_b for each specimen. For the specimen II3C where PZT_u and PZT_b are placed in a distance of 150 mm it is obvious that the behavior of those two transducers is totally different. On the contrary for the specimens II4C and IIIA3C where the transducers were placed in a distance smaller than 120 mm the variation of the admittance has the same behavior for the transducers PZT_u and PZT_b as it can be seen in Fig. 18. Hence the influence radius of each transducer is approximately 60 mm.

5. Conclusions

The PZT transducers employed for damage detection of the concrete substrate in reinforced concrete column specimens confined by FRP jackets perform very well if the FRP jacket consists of two layers, but fail to detect the damage if the number of the FRP layers increases. It is possible that when the PZT transducers fail to detect the damage of the concrete substrate, they operate as strain-gauges measuring the admittance due to the deformation of the jacket. Although this is only an initial study, the results indicate that the use of PZT transducers on FRP jackets for damage detection is a highly promising technique. However more research is necessary to be carried out concerning the specific topic.

Acknowledgments

This research has been co-financed by the European Union (European Social Fund-ESF) and Greek National Funds through the Operational Program “Education and Lifelong Learning” of the National Strategic Reference Framework (NSRF) – Research Funding Program: THALES – Investing in knowledge society through the European Social Fund. The authors wish to thank the students E. Choutopoulou, E. Fotaki, M. Skorda and M. Stathopoulou for their assistance in the experimental program.

References

- Akuthota, B., Hughes, D., Zoughi, R., Myers, J. and Nanni, A. (2004), “Near field microwave detection of disbond in fiber reinforced polymer composites used for strengthening concrete structures and disbond repair verification”, *J. Mater. Civil Eng. - ASCE*, **16**(6), 540-546.
- Bhalla, S. and Soh, C.K. (2003), “Structural impedance damage diagnosis by piezo-transducers”, *J. Earthq. Eng. Struct. D.*, **32**, 1897-1916.
- Bhalla, S. and Soh, C.K. (2004), “Health monitoring by piezo-impedance transducers I: modeling”, *J. Aerospace Eng.*, **17**, 154-165.
- Davor, M. and Richard, M., (1998), “Thermal imaging technique to detect delamination in CFRP plated concrete”, *SPI proceedings*, **3396**, 22-27.
- Dow Corning commercial site, <http://www.dowcorning.com/>
- EN 2561 (1995), *Carbon fibre reinforced plastics – Unidirectional laminates - Tensile test parallel to the fibre direction*, European Committee for Standardization, Brussels.
- Giurgiutiu, V., Harries, K.A., Petrou, M.F., Bost, J. and Quattlebaum, J. (2003), “Disbond detection with piezoelectric wafer active sensors in RC structures strengthened with FRP composite overlays”, *J. Earthq. Eng. Eng. Vib.*, **2**(2), 213-224.
- Giurgiutiu, V. and Xu, B. (2004), “Development of a field-portable small-size impedance analyzer for structural health monitoring using the electromechanical impedance technique”, *Proc. SPIE 5391, Smart Structures and Materials 2004: Sensors and Smart Structures Technologies for Civil, Mechanical, and Aerospace Systems*, doi: 10.1117/12.541343.
- Kim, S.D., In, C.W., Cronin, K.E., Sohn, H. and Harries, K.A. (2007), “A reference-free NDT technique for debonding detection in CFRP strengthened RC structures”, *J. Struct. Eng. - ASCE*, **8**, 1080-1091.
- Kim, S.B., Kim, J.H., Nam, J.W., Kang, S.H. and Byeon, K.J. (2008), “Bond-slip model of interface between CFRP sheets and concrete beams strengthened with CFRP”, *Korea Concrete Institute*, **20**(4), 477-486.
- Liang, C., Sun, F.P. and Rogers, C.A. (1994), “Coupled Electro-mechanical analysis of adaptive material systems determination of the actuator power consumption and system energy transfer”, *J. Intel. Mat. Syst. Str.*, **5**(1), 15-20.
- Oehlers, D.J. (2006), “Ductility of FRP plated flexural members”, *Cement Concrete Comp.*, **28**(10), 898-905.
- Overly, T.G., Park, G., Farinholt, K.M. and Farrar, C.R. (2009), “Piezoelectric active-sensor diagnostics and validation using instantaneous baseline data”, *IEEE Sens. J.*, **9**, 1414-1421.
- Park, S., Park, G., Yun, C.B. and Farrar, C.R. (2009), “Sensor self-diagnosis using a modified impedance model for active sensing-based structural health monitoring”, *J. Struct. Health Monit.*, **8**, 71-82.
- Park, G., Farrar, C.R., Scalea, F.L. and Coccia, S. (2006a), “Performance assessment and validation of piezoelectric active-sensors in structural health monitoring”, *Smart Mater. Struct.*, **15**(6), 1673.
- Park, G., Farrar, C.R., Rutherford, A.C. and Robertson, A.N. (2006b), “Piezoelectric active sensor self-diagnostics using electrical admittance measurements”, *J. Vib. Acoust.*, **128**(4), 469-476.

- Park S., Kim, J.W., Lee C. and Park, S.K. (2011), "Impedance-based wireless debonding condition monitoring of CFRP laminated concrete structures", *NDT&E Int.*, **44**, 232-238.
- Peairs, D, Grisso, B., Inman, D., Page, K., Athman, R. and Margasahayam, R. (2003), "Proof-of-concept application of impedance-based health monitoring on space shuttle ground structures", *NASA-TM-2003-211193*.
- Providakis, C.P., Stefanaki, K.D., Voutetaki, M., Tsompanakis, J. and Stavroulaki, M. (2013), "Damage detection in concrete structures using a simultaneously activated multi-mode PZT active sensing system: Numerical modelling", *Struct. Infrastruct. E.*, **10**(11), 1451-1468.
- Saafi, M. and Sayyah, T. (2000), "Health monitoring of concrete structures strengthened with advanced composite materials using piezoelectric transducers", *Composites: Part B*, **32**, 333-342.
- Triantafillou, T.C. (2001), "Seismic retrofitting of structures using FRPs", *Progress Struct. Eng. Mater.*, **3**(1), 57-65.
- Tseng, K.K.H. and Naidu, A.S.K. (2001), "Non-parametric damage detection and characterization using piezoceramic material", *Smart Mater. Struct.*, **11**, 317-329.
- Yang, Y., Hu, Y. and Lu, Y. (2008), "Sensitivity of PZT impedance sensors for damage detection of concrete structures", *Sensors*, **8**, 327-346.